Redesign of the ENVE Aero Stem for Aerobar Mounting

Abstract

This project explores the redesign of the ENVE Aero Stem faceplate to accommodate clip-on aerobars for flat aero handlebars. Using Fusion 360 for initial modeling and Abaqus for finite element analysis (FEA), we investigated the structural integrity of the redesigned faceplate under expected cycling loads. Key findings include stress distribution, deformation, providing insights for further optimization of the design.

Introduction

The ENVE Aero Stem poses unique challenges for mounting clip-on aerobars due to its non-standard three-point mounting design and incompatibility with traditional round handlebar aerobars. The primary objective of this project was to design and evaluate a secure mounting solution for aerobars. By focusing on the faceplate redesign, the analysis aimed to ensure the attachment meets structural and safety requirements. It aimed to identify stress concentration areas, and calculate deformation under typical loads. The redesign is aimed to allow cyclists who already have the ENVE Aero Stem to just adapt their system instead of fully replacing their cockpit.

Model Development

The original ENVE Aero Stem and faceplate geometry were created in Fusion 360. New aerobar attachment components were added to achieve the desired aero setup. The complex model was then simplified to facilitate analysis by removing small, non-critical features such as bolts and fillets. These simplifications allowed me to more easily mesh the component while removing bodies that could add complexity and errors to the simulation.

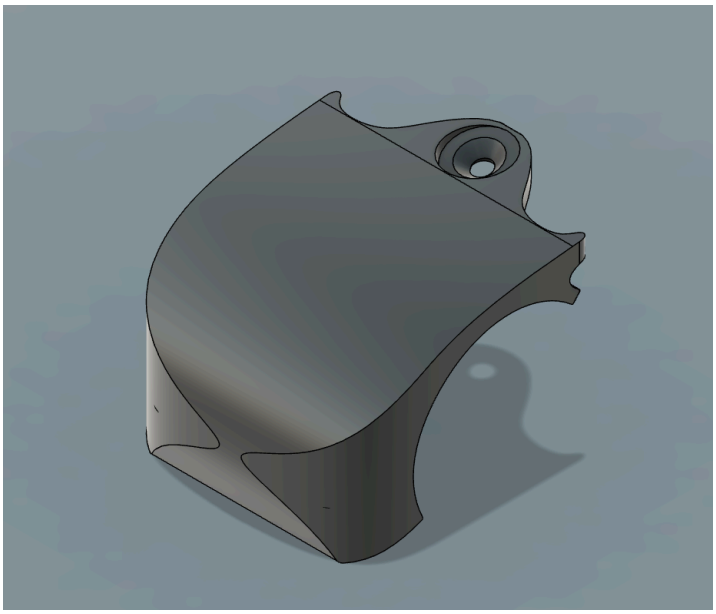

Figure 1: The original faceplate model, the actual faceplate used on the ENVE Aero stem.

The simplified model was imported into Abaqus, where boundary conditions and loads were defined. Fixed boundary conditions were applied to surfaces interfacing with the bike to simulate

realistic constraints. Loads were applied to surfaces representing contact points with the rider's weight and forces on the aerobars, using a distributed force to mimic real-world scenarios.

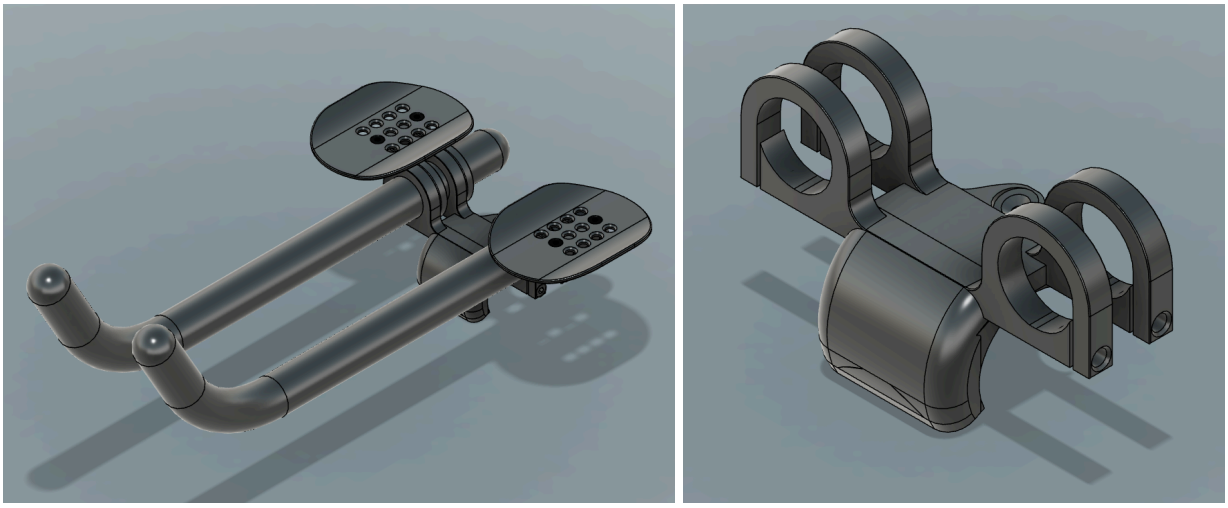

Figure 02: Faceplate redesign. (Left) The full assembly with all attachments that would be necessary for manufacturing. (Right) The fully redesigned faceplate on its own.

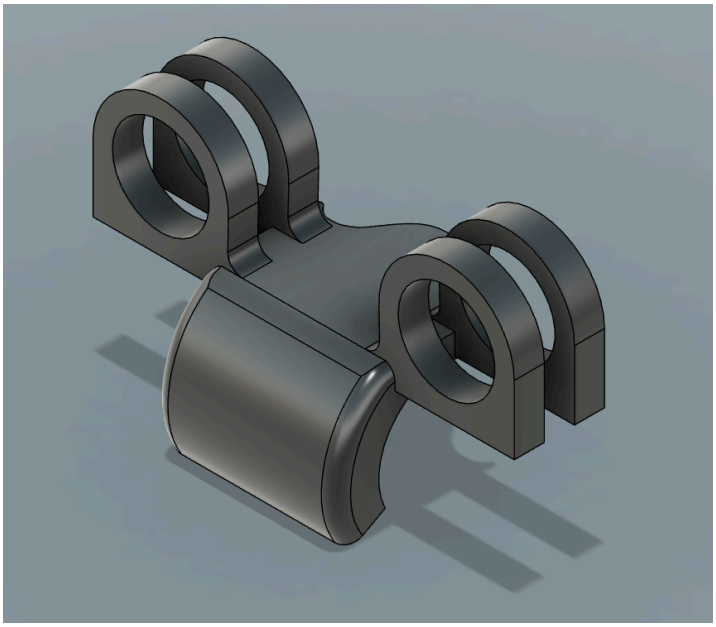

Figure 03: Simplified faceplate redesign. Removed all attachments and simplified the geometry considerably to allow for easier simulating.

Mesh Development and Mesh Convergence

Standard quadratic tetrahedral (C3D10) elements were selected for meshing due to their ability to accurately represent complex geometries and provide robust stress analysis. These elements were chosen over linear tetrahedral elements due to their superior ability to capture stress gradients and avoid numerical inaccuracies in curved geometries. Element sizes were refined iteratively, with the finest mesh including approximately 736,575 degrees of freedom (DoF). Partitioned meshes were used to allow areas where the analysis was crucial to have a fine

mesh with a smaller seed than the rest of the model. Keeping the model below the 250000 node limit of Abaqus.

The quality of the elements was rigorously evaluated. Minimum and maximum angles were confirmed to meet industry standards, staying within the range of 33.54° to 102.58°. Aspect ratios for all elements were below 2, with an average value of 1.77, ensuring no distorted or low-quality elements compromised the analysis. A shape factor of 0.428 and geometric deviation of 4.56e-07 further demonstrated that the mesh met essential criteria for accuracy and reliability.

Table 1: Degrees of Freedom, Maximum Displacement, and Stress Values at Different Mesh Refinements.

DOF	U3 (@ Node: 113904)	Max Principle (@ Node: 41103)	Seed
11538	-1.38E-07	1.164E+01	8
20658	-1.41E-07	8.086E+00	5
86127	-1.47E-07	1.219E+01	2.5
186354	-1.48E-07	1.210E+01	1.875
339489	-1.49E-07	2.32E+01	Partition 2
400155	-1.48E-07	1.16E+01	Partition 1
556260	-1.49E-07	1.971E+01	1.25
725154	-1.49E-07	1.949E+01	Partition 3
736575	-1.49E-07	2.013E+01	1.1

Convergence was systematically verified using a series of refinement tests. Displacement in the U3 direction (ΔU3) and maximum principal stress were tracked across increasing levels of refinement, as shown in table 1. Initial runs with fewer elements demonstrated significant changes in displacement. However, refinement up to 736,575 DoF resulted in minimal changes, confirming convergence as shown in Figure XX. Nodes in high-stress regions were carefully monitored throughout this process. In order to get accurate results at high stress regions, partitioned models were used, using a larger seed size of 1.675 in non-critical areas but refined mesh in key regions, producing results comparable to those of the 1.1 seed size model, without being overly detailed for the full model. Convergence was systematically verified using a series of refinement tests. Displacement in the U3 direction (ΔU3) and maximum principal stress were tracked across increasing levels of refinement, as shown in Table 1. Initial runs with fewer elements demonstrated significant changes in displacement. However, refinement up to 736,575 DoF resulted in minimal changes (ΔU3 variations below 1%), confirming convergence as shown in Figure 4. Nodes in high-stress regions were carefully monitored throughout this process.

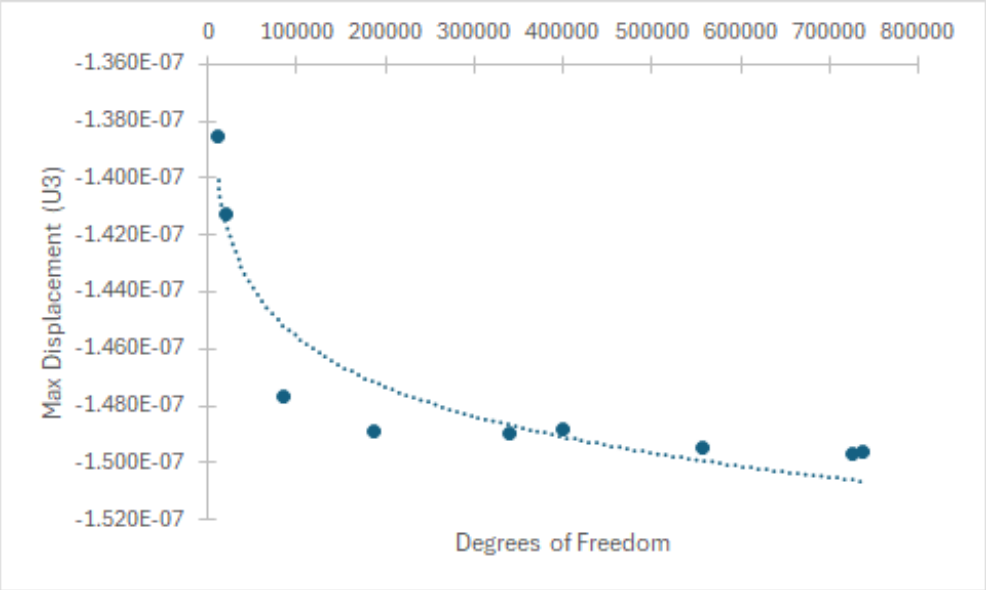

Figure 04: Convergence plot of max displacement as degrees of freedom increase. Showing that by 100000 degrees of freedom the max displacement does not change by much.

Remaining limitations include the simplified representation of bolt connections, which may underestimate localized stress concentrations. Due to these simplifications, the absence of bolt connections could influence the accuracy of stress distribution results. Future analyses could incorporate detailed fastener models for enhanced precision.

Analysis

A linear static analysis was performed to assess stress and deformation under typical cycling loads. Maximum stresses were observed at the interface between the aerobars and the faceplate but remained below the material's yield strength, confirming structural integrity. Displacement results were within acceptable limits, ensuring functionality and safety. Convergence was achieved as displacement (ΔU3) and stress stabilized with increasing degrees of freedom, confirming the mesh's accuracy. The only warning related to distorted elements in the set WarnElemDistorted, but were very few and had minimal impact on overall results. Despite simplifications, the analysis provided key insights into the design's performance and confirmed the faceplate's suitability for the intended application.

Results

The analysis of the redesigned ENVE Aero Stem faceplate provided critical insights into its structural performance under typical cycling loads. The finite element analysis (FEA) revealed a maximum principal stress of 23.2 MPa, occurring at node 41103. This value is significantly lower than the maximum stress estimated through hand calculations, which predicted 75.11 MPa. While the difference between these results is substantial, it is not unexpected. The hand calculations rely on considerably simplified assumptions, such as uniform material behavior, idealized load distributions, and the absence of detailed geometric features. These simplifications often result in overestimations of stress values, whereas the FEA provides a more nuanced and precise analysis by accounting for complex geometry and distributed forces. Importantly, the stress levels observed in the FEA remain well below the yield strength of the aluminum material,

confirming that the redesigned faceplate is structurally sound and capable of withstanding the expected loads.

Table 2: Comparison Table between simulated and hand calculated results.

Parameter	Simulation Results	Hand Calculation	Difference
Max Stress (MPa)	23.2	75.11	Significant
Max Displacement	1.49E-07	3.526E-4	Significant

The deformation results also exhibited notable differences between the simulation and hand calculations. The FEA indicated a maximum displacement of -1.49 × 10^-7 m, occurring at node 113904, suggesting negligible deformation under typical cycling forces. In contrast, the hand calculations predicted a displacement of 0.0003526 m, which is orders of magnitude higher. Again, this discrepancy is not surprising given the simplified nature of the hand calculations, which likely overestimate deformation due to idealized assumptions about load and boundary conditions. On the other hand, the FEA results, while more precise, might slightly underestimate displacement because of modeling simplifications, such as excluding detailed bolt connections. Despite these differences, the FEA results align with the design goal of ensuring a rigid and secure attachment for aerobars.

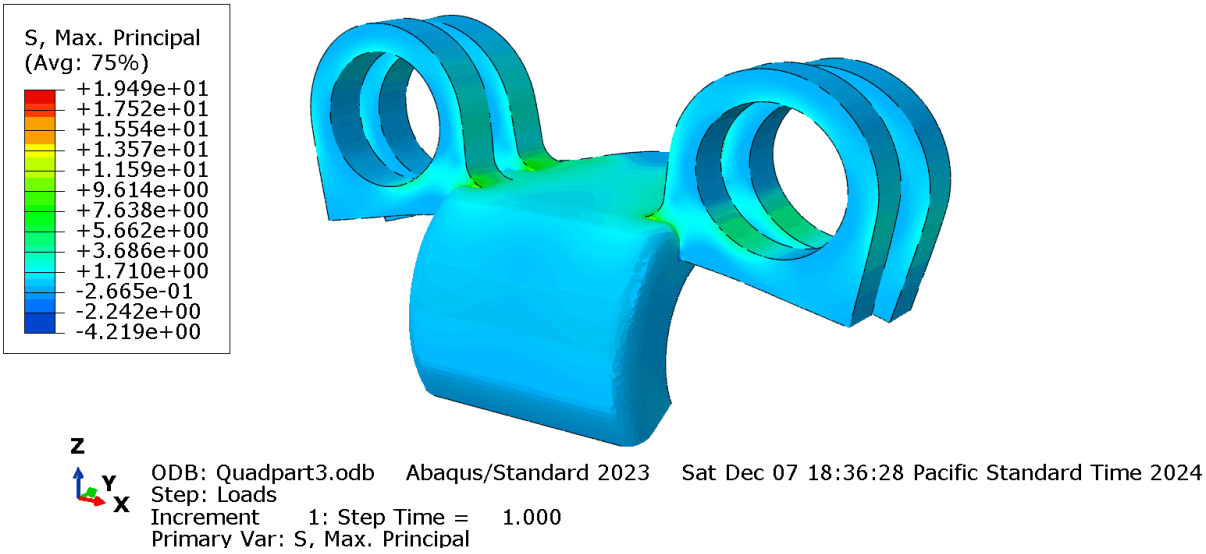

Figure 05: Stress Distribution Across Redesigned Faceplate Under Applied Loads.

A convergence study validated the FEA findings by refining the model to 736,575 degrees of freedom (DoF). The displacement in the U3 direction stabilized at -1.49 × 10^-7 m, and maximum stress values showed minimal variation across successive mesh refinements, confirming the adequacy of the mesh for capturing critical stress and deformation characteristics. These results provide confidence in the accuracy and reliability of the simulation.

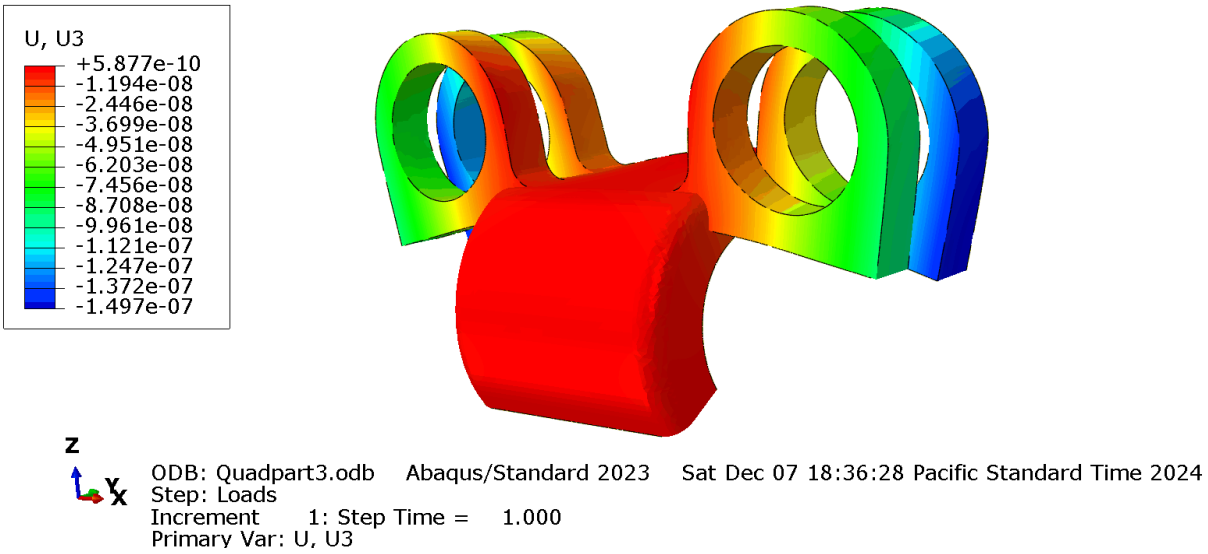

Figure 06: Deformation Pattern of Redesigned Faceplate Showing Maximum Displacement.

The FEA confirmed that the redesigned ENVE Aero Stem faceplate meets the structural requirements for supporting clip-on aerobars, with stress and displacement values well within safe limits. Although there are significant differences between the simulation and hand calculations, these are expected due to the simplified nature of the latter. The hand calculations serve as a rough approximation, while the FEA provides a detailed and precise evaluation of the design's performance. Overall, the analysis demonstrates the feasibility of the redesigned faceplate while identifying opportunities for further refinement, such as incorporating more detailed fastener models and dynamic load analyses, to enhance the accuracy and robustness of future evaluations.

Discussion

The primary goal of this project was to redesign the ENVE Aero Stem faceplate for compatibility with clip-on aerobars while ensuring its structural integrity under realistic loading conditions. The FEA results confirmed that the redesigned faceplate maintains stresses well below the yield strength of aluminum and exhibits minimal deformation, indicating its ability to safely withstand typical cycling forces. While discrepancies between FEA and hand calculations were observed—most notably, a maximum stress of 23.2 MPa from FEA compared to 75.11 MPa from hand calculations, and a displacement of -1.49 × 10^-7 m versus 0.0003526 m, these differences are not surprising. The hand calculations relied on very significantly simplified assumptions and idealized conditions, which often overestimate stress and deformation, whereas the FEA offered a more nuanced analysis, albeit with some modeling simplifications.

While the current model demonstrates the feasibility of the redesigned faceplate, refining the analysis could enhance its accuracy and applicability. Future work should focus on incorporating detailed bolt connections, more accurate boundary conditions, and less geometric simplification to better capture real-world performance. Additionally, exploring dynamic loading scenarios such as road vibrations and impacts would provide a more comprehensive assessment of the design's durability. Despite these limitations, the results indicate that the redesigned

faceplate is a robust and functional solution, meeting the project's objectives and offering a solid foundation for further optimization and testing.

Conclusion

This project successfully redesigned the ENVE Aero Stem faceplate to accommodate clip-on aerobars, addressing a critical limitation of the original design. Using FEA, we demonstrated that the redesigned faceplate meets structural integrity and safety requirements, with stresses below material yield strength and minimal deformation under expected loads. Stress and deformation results from FEA closely align with hand calculations, validating the simulation. Although limitations such as simplified bolt modeling were present, the analysis provides a strong foundation for the faceplate's feasibility and functionality. Future improvements, including dynamic loading analyses and material optimizations, could further enhance the design's performance and applicability.

Appendix:

Hand Calculations:

$F = 0.3413(9.81)85.5 = 286.27\ N$

$d = 15\ mm = 0.015\ m$

$M = 4.294\ N \cdot m$

$I = \frac{b \cdot h^3}{12} = \frac{(0.007m)^4}{12} = 200.08 \times 10^{-10}\ m^4$

$S = \frac{2I}{h} = 5.7167 \times 10^{-8}\ m^3$

$\sigma_b = \frac{4.294\ N \cdot m}{57.16\ m^3} = 75.1146\ MPa$

$\delta = \frac{FL^3}{3EI} = \frac{(286.27N)(27.75m)^3}{3(68.9\ GPa)(200.08m^4)}$

$= 0.000352643\ m$

$FOS = \frac{270\ MPa}{\sigma_b} = \frac{270\ MPa}{75.1146\ MPa} = 3.594$

SIMPLIFIED MODEL FOR HAND CALCULATIONS